JOC*Article*

One-Pot Synthesis of Helical Aromatics: Stereoselectivity, Stability against Racemization, and Assignment of Absolute Configuration Assisted by Experimental and Theoretical Circular Dichroism

Masashi Watanabe,[†] Hiroshi Suzuki,[†] Yasutaka Tanaka,*[,†] Toshimasa Ishida,[‡] Tatsuo Oshikawa,[§] and Akiyoshi Tori-i[⊥]

Department of Materials Science, Shizuoka University, Hamamatsu, Shizuoka 432-8561, Japan, Institute for Molecular Science, Okazaki, Aichi 444-8585, Japan, Numazu College of Technology, 3600 Ooka Numazu 410-8501, Japan, and Saga University, Honjo-machi 1, Saga 840-8502, Japan

tcytana@ipc.shizuoka.ac.jp

Received July 6, 2004

Helical aromatics (**1**) were synthesized via one step in good quantity by solvent-free condensation of *N*,*N*′-*p*-phenylenediamine (**2**) and various carboxylic acids in the presence of a Lewis acid. Microwave irradiation greatly facilitated the condensation reaction to furnish **1** with a 100% diastereo- and a 50% enantioselectivity, when a chiral carboxylic acid was utilized. **1f**, derived from 2-methylglutaric acid, was quite stable, no racemization taking place even at 200 °C. The assignment of the absolute configurations to the helical aromatics has been achieved by experimental and theoretical CD spectra calculated by time-dependent density functional theory.

Introduction

13,14-dialkyldibenzo[*b*,*j*][4,7]-phenanthroline (**1**) possesses a twisted conjugated aromatic plane due to steric hindrance from two alkyl groups at the 13 and 14 positions giving rise to helical chirality.[1] Thus, **1** and its derivatives could be considered as a new class of helical aromatics.

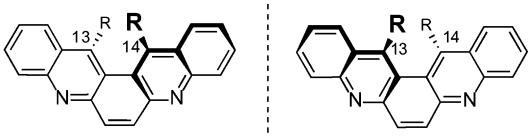

On one hand, the helical aromatics such as helicenes, which also present left- and right-handed chiral helical structure, have been intensively studied for their chiroptical and photochromic properties,[2] as well as in asymmetric molecular recognition, synthesis, sensors, and polymer fields.[3] Recently, their self-assembled structures have also drawn attention because of their unique physical properties, including liquid crystallinity and nonlinear optical responses.[4] The potential use of such aromatics largely depends on obtaining them in good quantity and in an enantiomerically pure form. Once isolated, the homochiral forms should strongly resist racemization. However, the synthetic complexity of these aromatics, involving multistep reactions and the chiral resolution, still impedes their production in quantity. In addition such helical conjugated aromatics racemize easily especially at high temperatures. We have previously demonstrated that **1** (R = CH_3) was synthesized via a solvent-free one-pot condensation reaction of *N*,*N*′-diphenyl-*p*-phenylenediamine (**2**) with carboxylic acids (**3**) in the presence of $ZnCl_2$ as Lewis acid.[5] Here we report that a variety of derivatives of **1** possessing different alkyl substituents at the 13 and 14 positions have also been obtained in one pot by conventional heating as well as by microwave irradiation. Microwave irradiation drastically shortened the reaction time and brought about stereoselectivity. We have also revealed that several

* To whom correspondence should be addressed. Phone: +81-53-478-1164. Fax: +81-53-478-1199.
† Shizuoka University.
‡ Institute of Molecular Science.
§ Numazu College of Technology.
⊥ Saga University.

(1) 5,8-Diazapentaphene rings (dibenzo[*b*,*j*][4,7]-phenanthroline) have been known since the 1950s; see: (a) Badger, G. M.; Pettit, R. *J. Chem. Soc.* **1952**, 1874. (b) Hellwinkel, D.; Ittemann, P. *Liebigs Ann. Chem.* **1985**, 1501.

(2) For a review of aromatic helical molecules, see: (a) Wynberg, H. *Acc. Chem. Res.* **1971**, *4*, 65. (b) Martin, R. H. *Angew. Chem., Int. Ed. Engl.* **1974**, *13*, 649. (c) Laarhoven, W. H.; Prinsen, W. J. C. *Top. Curr. Chem.* **1984**, *125*, 63. (d) Meurer, K. P.; Vögtle, F. *Top. Curr. Chem.* **1985**, *127*, 1. For a review of chiroptical properties, see: (e) Grimme, S.; Harren, J.; Sobanski, A.; Vögtle, F. *Eur. J. Org. Chem.*, **1998**, 1491.

(3) (a) Murguly, E.; McDonald, R.; Branda, N. R. *Org. Lett.* **2000**, *2*, 3169. (b) Sato, I.; Yamashima, R.; Kadowaki, K.; Yamamoto, J.; Shibata, T.; Soai, K. *Angew. Chem., Int. Ed.* **2001**, *40*, 1096. (c) Reetz, M. T,; Sostman, S. *Tetrahedron* **2001**, *57*, 2515. (d) Schmuck, C. *Angew. Chem., Int. Ed.* **2003**, *42*, 2448. (e) Urbano, A. *Angew. Chem., Int. Ed.* **2003**, *42*, 3986.

(4) (a) Katz, T. J. *Angew. Chem., Int. Ed.* **2000**, *39*, 1921. (b) Verbiest, T.; Sioncke, S.; Persoons, A.; Vyklicky, L.; Katz, T. J. *Angew. Chem., Int. Ed.* **2002**, *41*, 3882.

(5) (a) Tanaka, Y.; Sekita, A.; Suzuki, H.; Yamashita, M.; Oshikawa, T.; Yonemitsu, T.; Torii, A. *J. Chem Soc., Perkin Trans. 1* **1998**, 2471. (b) Tanaka, Y.; Sekita, A.; Suzuki, H.; Torii, A. U.S. Patent 5973151, 1999.

10.1021/jo048858k CCC: $27.50
Published on Web 10/20/2004

SCHEME 1. Formation of 1 from 2 and (a) Carboxylic Acid or (b) Dicarboxylic Acid

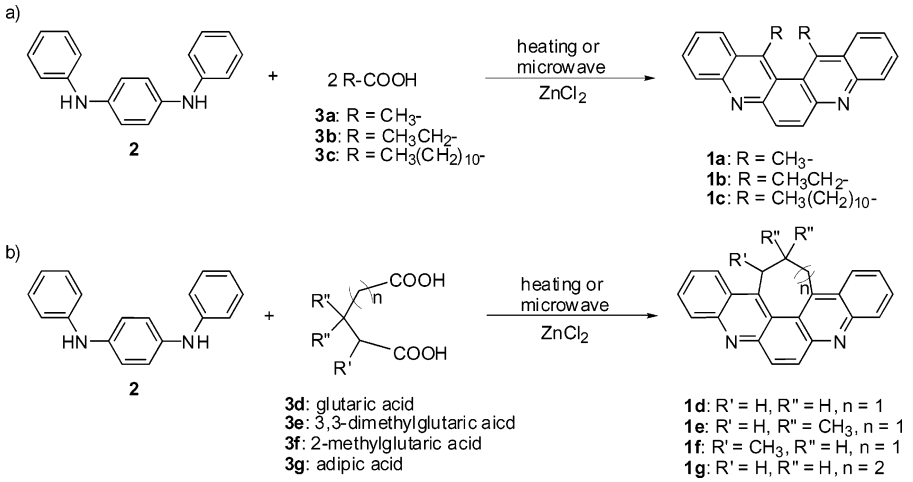

TABLE 1. Reaction Time and Yields of Helical Aromatics (1) from 2 and Carboxylic Acid (3)

	reaction time (min)		yield (%)		
carboxylic acid	heating	microwave	heating	microwave	product
3a	540	30	56	35	**1a**
3b	540	30	50	0	**1b**
3c	540	30	0	<1	**1c**
3d	540	5	78	83	**1d**
3e	540	5	80	84	**1e**
3f	540	5	18	34	**1f**[a]
3g	540	5	0	<1	**1g**

[a] When started with optically pure (*S*)-**3f** and **2**, both conventional heating and microwave irradiation gave the same yields as those starting with racemic **3f**.

derivatives of **1** could be resolved into their respective enantiomers, some of which are quite stable as such. No racemization takes place even at high temperature, as the bulkiness of the substituents exerts a large influence on the racemization barrier. The assignment of the absolute configurations to the helical aromatics has been achieved by experimental and theoretical CD spectra calculated by time-dependent density functional theory.

Results and Discussion

Synthesis of Helical Aromatics (1). In a typical preparation, a mixture of *N*,*N*′-diphenyl-*p*-phenylenediamine (**2**) and a carboxylic acid such as acetic acid (**3a**) in the presence of an excess of $ZnCl_2$ was placed in a three-necked flask equipped with a mechanical stirrer, thermometer, and reflux condenser. The mixture was stirred and heated with an oil bath at 200 °C for 9 h, giving rise to a dark and viscous resinous substance. Soxhlet extraction with $CHCl_3$ for 12 h and subsequent column chromatography (silica gel, $CHCl_3$) of the concentrated extract afforded **1a** (56%), together with a small amount of **4a** (<1%) and **5a** (≪1%) (Scheme 1).[4] Compounds **4a** and **4b** can also be quantitatively provided by the reduction of **1a** and **1b** with $LiAlH_4$ in diethyl ether. Microwave irradiation, instead of conventional heating with an oil bath, greatly reduced the reaction time. The synthetic procedure is almost identical with that of conventional heating: the mixture of starting materials, in a round-bottom flask equipped with reflux condenser, was placed in a domestic microwave oven (2.45 GHz, 500 W) and irradiated. The reaction progress was monitored by thin-layer chromatography (SiO_2, $CHCl_3$/ethyl acetate = 8/1). For example, **1d** was provided in a 83% yield by microwave irradiation for 5 min, while conventional heating for 9 h afforded a 73% yield (Table 1). However, carboxylic acids possessing low boiling points such as acetic (**3a**) and propionic (**3b**) acids caused bumping upon microwave irradiation resulting in decreased chemical yields (Table 1). Only trace amounts of condensation products of **1c** and **1g** were obtained from lauric (**3c**) and adipic (**3g**) acids probably because of the higher bulkiness of alkyl or methylene groups.

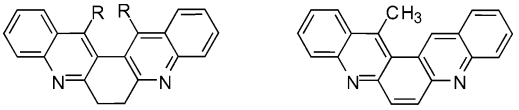

The mechanism of acridine synthesis from diphenylamine and a carboxylic acid in the presence of Lewis acid has been established and suggested to account for that of formation of **1**.[6] Thus, N-acylation of **2** with carboxylic acids resulting in mono- and di-N-acylated forms of **6** and **6′**, followed by the acyl group transfer to an adjacent aromatic carbon, provided aryl ketones of **7** and **7′**, and subsequent cyclodehydration gave rise to acridine derivatives of **8** and **8′**. **8** readily underwent N-acylation, giving **8′** (Scheme 2). In particular, **6c** and **6c′** could be detected by mass spectrometry in the initial stage of the reaction (<15 min) and **8c** and **8c′** could be isolated, and their structures were also determined by high-resolution mass spectrometry and ^{1}H NMR spectroscopy.[7] **6a′** obtained from the reaction of **2** with acetic anhydride could be readily converted into **1a** in a 78% yield, also indicating that the one-pot reaction of **2** with **3** giving **1** proceeds through *N*-acyl intermediates (Scheme 3).[8] It seems the second acyl transfer in **8′** occurred preferentially at the aromatic carbon denoted as α, leading to **9**α, and the

(6) For the reaction mechanism for 9-substituted acridines from diphenylamine and carboxylic acid, see: (a) Tsuge, O.; Nishinohara, M.; Tashiro, M. *Bull. Chem. Soc. Jpn.* **1963**, *36*, 1477. (b) Bernthsen, A. *Justus Liebigs Ann. Chem.* **1884**, *1*, 224.

SCHEME 2. Proposed Mechanism for Formation of 1 from 2 and Carboxylic Acid (3)

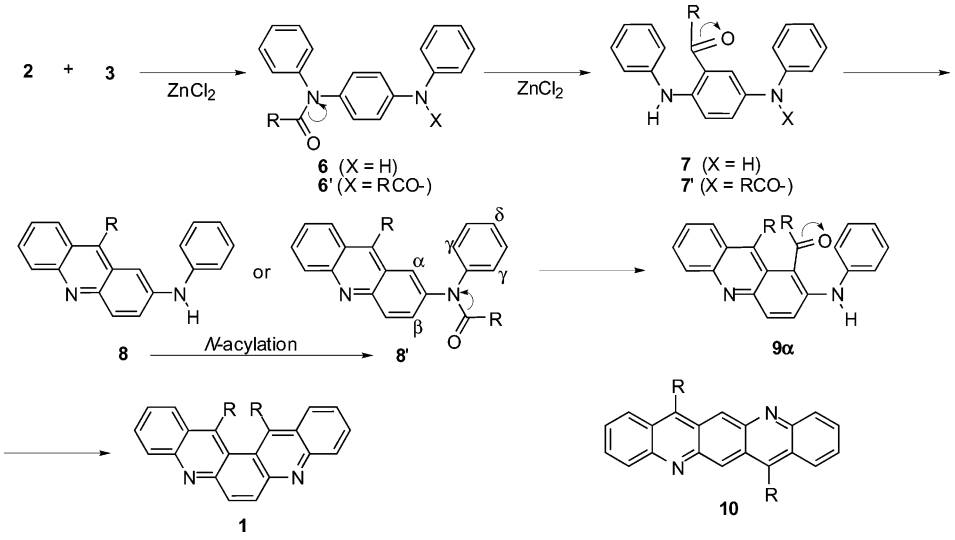

SCHEME 3. Stepwise Formation of 1a through 6a

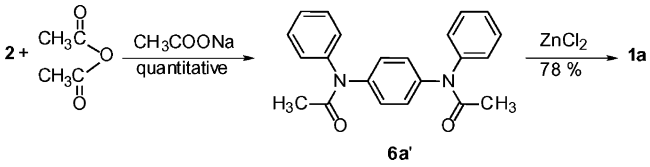

following cyclodehydration affords **1** as the single condensation product. In particular, the α carbon among four aromatic carbons (α, β, γ, and δ) in **8′** possesses the highest HOMO density (α = 0.104, β = 0.014, γ = 0.020, δ = 0.032), which were calculated by a MOPAC/PM5 wave function, indicating that the electrophilic acyl cation attacks the α position in preference to the others.[9] This is also the reason a flat condensed aromatic of **10** derived through **9**β was not obtained even if **10** is far less strained as compared with **1**. The mechanisms of formation of dihydro form (**4a**) of **1a** and the monomethyl form (**5a**) have remained obscure: presumably, hydrogenation and the C−C bond cleavage between one of the methyls and the aromatic carbon in **1a** occur to relax the highly strained conjugated aromatic ring to afford **4a** and **5a**, respectively.

Chiral Resolution and Kinetic Parameters for Racemization. 1a (R = CH_3−) and **1b** (R = CH_3CH_2−) were resolved into the respective enantiomers by chiral HPLC separation. For **1a**, the pronounced tailing and leading of first and second chromatographic peaks, respectively, showed a tendency toward racemization during chiral separation, while **1b** was fully optically resolved (Figure 1). **1d** and **1e**, which contain a trimethylene bridge between the 13 and 14 positions, could not be optically resolved under various separation conditions, probably due to the greater flexibility resulting from the

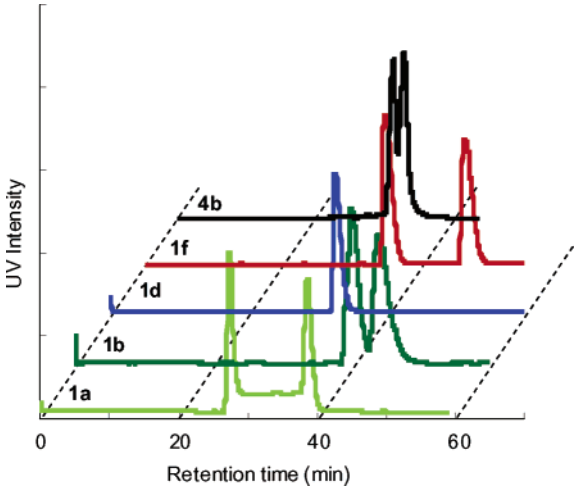

FIGURE 1. Chiral HPLC separations of **1a**, **1b**, **1d**, **1f**, and **4b**. Column: DAICEL OJ-R; Solvent: acetonitrile/H_2O = 3/7. Detector: UV at 254 nm.

bridges. On the other hand, **1f**, which also possesses a trimethylene bridge as well as an sp^3 chiral carbon in the bridge, could be conveniently separated into enantiomers (Figure 1). Optically resolved enantiomers of **1** showed characteristic CD spectra reciprocal to one another: CD spectra of a pair of enantiomers of **1f** are shown in Figure 2. **4b** could also be separated into a pair of enantiomers without racemization during the separation.[10]

The rates of racemization of **1a**, **1b**, **1f**, and **4b** were estimated by the time-course of CD spectra at different temperatures: the spectral change in the first eluate of **1a** at 45 °C was shown in Figure 3. The racemization process in **1a** and **1b** follows first-order kinetics with respect to the concentration (eq 1);

$$[(P) - \mathbf{1}] \underset{k_{-1}}{\overset{k_1}{\rightleftharpoons}} [(M) - \mathbf{1}] \qquad (1)$$

(7) Molecular ion peaks (MH^+) of **6c**, **6c′**, **8c**, and **8c′** were observed at 443.3061 (calcd 443.3062), 625.4740 (calcd 625.4733), 425.2953 (calcd 425.2957), and 607.4628 (calcd 607.4627), respectively, under high-resolution conditions. These mass spectra and ^1H NMR spectra of **8c** and **8c′** are shown in Supporting Information.

(8) *N*1,*N*4-Diphenyl-1,4-benzenendiamine and *N*1-[4-methyl(phenyl)-carboxamidophenyl]-*N*1-phenylacetamide are in the IUPAC nomenclature of **2** and **6a′**.

(9) HOMO density is equal to the square of the orbital coefficient of the p_Z component; see also Experimental Section.

(10) Experimental as well as theoretical CD spectra of **1a** and **4a** have shapes identical to those of **1b** and **4b**, respectively, which are not unexpected from close structural similarities.

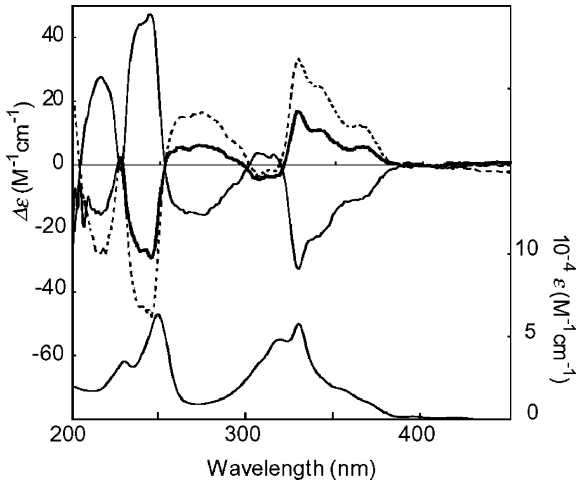

FIGURE 2. CD spectra (top) of optically resolved **1f**: first eluate (solid line), second eluate (dotted line), and **1f** synthesized from (*S*)-2-methylglutaric acid ((*S*)-**3f**) by microwave irradiation (bold, 50.3% enantiomeric excess). Absorption spectrum (bottom) of **1f**. Scale on the right abscissa is for the absorption spectrum. All spectra were measured at 25 °C in methanol.

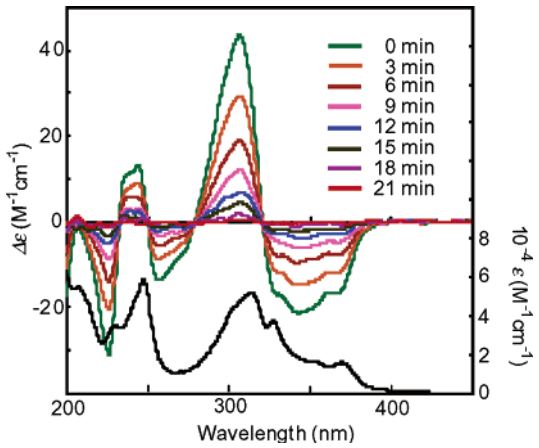

FIGURE 3. Time course of CD spectra (top) of the first eluate of **1a** measured at 45 °C in methanol.[10] Absorption spectrum (bottom) of **1a**. Scale on the right abscissa is for the absorption spectrum.

kinetic parameters, $\Delta H^{\ddagger}$ and $\Delta S^{\ddagger}$, derived from rate constants (k_1) are summarized in Table 2. In contrast the obvious alterations in CD intensity at various temperatures up to 200 °C were not observed for **1f** and **4b**, indicating that no racemization was occurring even at elevated temperatures. Table 2 also included theoretical parameters of $\Delta\Delta H_f^0$ as an index of racemization barrier calculated by molecular orbital methods.[11]

The experimental kinetic parameters were well reproduced by the theoretical parameters and also consistent with the chiral separation behaviors (Table 2 and Figure 1). These indicated that the bulkiness of the substituents exerts a large influence on the racemization barrier: thus, $\Delta H^{\ddagger}$ increases as smaller groups at 13 and 14 positions are substituted by larger ones (**5a** (monomethyl) < **1a** (dimethyl) < **1b** (diethyl)). The small differences in enthalpy ($\Delta H^{\ddagger}$ and $\Delta\Delta H_f^0$) for both experimental and theoretical values in **1d** and **1e** have also proven them to be racemized easily due to the greater flexibility in their trimethylene bridge. However, the high racemization barrier experimentally observed in **1f** was entirely unexpected, although **1f** also contains the trimethylene bridge. The theoretical $\Delta\Delta H_f^0$ of 47.9 kJ/mol for **1f** is too small to explain the barrier observed: the racemization of **1f** probably proceeded by way of a different transition conformation from the other **1** derivatives. No racemization of **4b** took place, even at 200 °C: the presence of a central hydrocarbon ring in helical aromatics generally increases the racemization barrier as compared with that of the parent fully aromatic derivatives.[12]

TABLE 2. Experimental and Theoretical Kinetic Parameters for Racemization of 1, 4, and 5

	experimental		theoretical (PM5)
helical aromatics	$\Delta H^{\ddagger}$ (kJ/mol)	$\Delta S^{\ddagger}$ (kJ/mol)	$\Delta\Delta H_f^0$ (kJ/mol)
1a	87.5	−24.1	77.6
1b	97.1	−26.9	100.1
1d	*a*	*a*	29.0
1e	*a*	*a*	40.8
1f	nd[b]	nd[b]	47.9
4b	nd[b]	nd[b]	121.8
5a	*a*	*a*	11.6

[a] Experimental parameters could not be obtained because homochiral forms were not available. [b] Nd means that the racemization was not detected in the temperature range of 25−200 °C.

^{1}H NMR Spectra and X-ray Single-Crystal Analyses of 1. The pronounced stability of **1f** against racemization is quite unique and can be ascribed to its structural characteristics. ^{1}H NMR spectrum of **1f** indicated five independent resonances assigned to five protons at the 13, 14, and 15 positions in the temperature range from −45 to 100 °C (Figure 4 and its inset) due to the immobilized methylene bridge and the conjugated aromatic ring as well. On the other hand, **1d** exhibited only two resonances for six protons at the 13, 14, and 15 positions in the same temperature range (inset in Figure 4), indicating the occurrence of fast ring inversion (racemization). The extra methyl group at the 13 position in **1f** appears to exhibit an anchoring effect to immobilize the methylene bridge, eventually preventing aromatic ring inversion. The specific NOEs between the protons at the 12 and 13, CH_3 and 14, and 1 and 15 positions observed in **1f** also confirmed restricted flexibility in the methylene bridge.

X-ray single-crystal analyses of the helical aromatics demonstrated that the conjugated aromatic rings are indeed twisted. The space-filling representations of racemic crystals of **1b** and **1f** are shown in Figure 5. The (*P*)- and (*M*)-enantiomers, which are mirror images of

(11) Theoretical $\Delta\Delta H_f^0$ is the difference in ΔH_f^0 between the most stable and transition state conformations. MOPAC/PM5 calculation always generated U-shape structures of helical aromatics **1** possessing C_s symmetry as the transition state conformation for racemization of **1**, while **1** in the most stable state took C_2 symmetry; see also Experimental Section. In particular, a racemization mechanism through the C_s-symmetric conformation in the transition state has been proposed by molecular orbital methods of AM1, MNDO, and PM3 to account for racemization of helicenes; see: Janke, R. H.; Haufe, G.; Würthwein, E.-U.; Borkent, J. H. *J. Am. Chem. Soc.* **1996**, *118*, 6031.

(12) (a) Goedicke, C.; Stegemeyer, H.; *Tetrahedron Lett.* **1970**, *11*, 937. (b) Carreño, M. C.; Carcía-Cerrada, S.; Urbano, A. *J. Am. Chem. Soc.* **2001**, *123*, 7929.

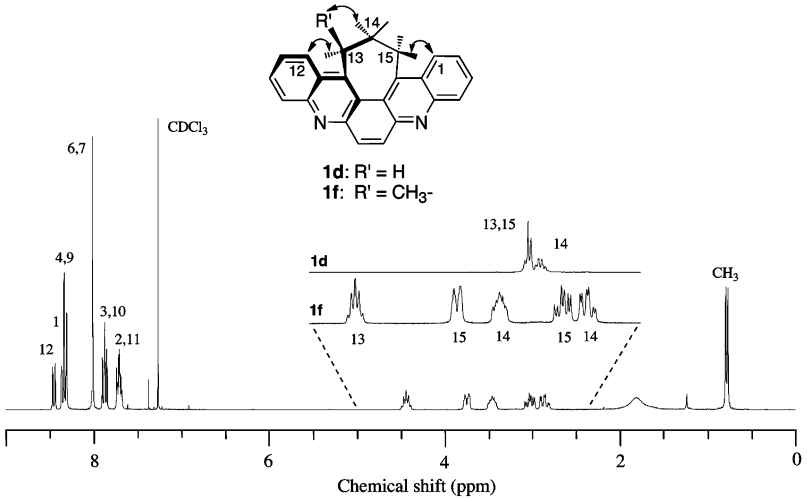

FIGURE 4. ^{1}H NMR spectrum of **1f** in $CDCl_3$ at 0 °C. The insets show the spectra expansions in the region of 2.50−4.75 ppm of **1f** (bottom) and **1d** (top). The numerals under the respective resonances in the insets indicate the proton positions in **1f** and **1d**. The arrows in the chemical structure stand for proton-to-proton NOEs.

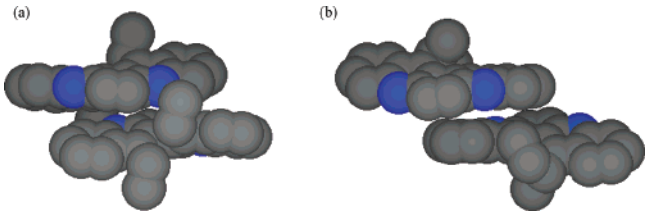

FIGURE 5. Space-filling renderings from the single-crystal X-ray diffraction data of racemic (a) **1b** and (b) **1f** consisting of pairs of (*P*)- and (*M*)-forms and (*S*)−(*M*)- and (*R*)−(*P*)-forms, respectively. Hydrogen atoms are omitted for clarify.

each other, were aligned alternately so as to form the racemic crystal. Only two isomers, a pair of enantiomers of (*S*)−(*M*)- and (*R*)−(*P*)-**1f**, were found to exist out of four possibilities, the other two being (*S*)−(*P*)- and (*R*)−(*M*)-**1f** (Figure 5b).[13] Therefore, the synthetic reaction of **1f** from racemic 2-methylglutaric acid (**3f**) and **2** proceeded diastereoselectively, and thus the point chirality at the terminal of the methyl group determines the helicity. The X-ray analysis of **1f** also indicated that the protons between 12 and 13 and between 1 and 15, respectively, are in close proximity.

Enantioselective Formation of 1f Assisted by Microwave Irradiation. Microwave-assisted reactions take place when a polar molecule coexists as solvents, catalysts, or reactants themselves. It is known that the frequency of the microwave radiation (2.45 GHz) does not activate specific bonds in an organic molecule. Nevertheless the coupling of microwaves with the dipolar molecule leads to a dielectric heating effect to directly heat the reactants and eventually accelerate a chemical reaction. Therefore, it has been argued that conventional heating and microwave-activated reactions share in general the identical reaction mechanism.[14] When started with optically pure (*S*)-**3f** and **2** in the presence of $ZnCl_2$, the conventional heating reaction gave a racemic mixture of **1f** as in the case starting with racemic **3f**; racemization of the sp^3 chiral carbon adjacent to carbonyl group in (*S*)-**3f** or in reaction intermediates seemed to take place through an enol form at elevated temperature. In marked contrast to conventional heating, microwave irradiation has achieved a 50.3% enantiomeric excess to give preference to one of the **1f** enantiomers over the antipode.[15] The product exhibited the same signs in the CD as those of the second eluate on HPLC chiral resolution of **1f** racemates (Figure 2). A shortening of the reaction period seemed to suppress racemization of the sp^3 chiral carbon and thus brought about enantioselectivity along with diastereoselectivity. The infrared radiation thermometer indicated that the temperature of the reaction mixture reached over 200 °C within 50s after commencing microwave irradiation. The rapid increase in temperature led the reactive starting materials and intermediates readily to the final products without racemization of the sp^3 carbon resulting in stereoselectivity. Repeated recrystallization from the enantiomer excess solution readily provided an enhancement of the optical purity of **1f**.

Assignment of Absolute Configuration of Helical Aromatics. The absolute configurations of helical aromatics were assigned on the basis of CD exciton chirality method (exciton-coupled CD) as well as comparison between experimental and theoretical CD spectra generated by Gaussian 03. Exciton-coupled CD is based on interacting choromophores, which bring about the exciton splitting of electric transition of the chromophores.[16] When the two choromophores are oriented with clockwise movement from front to back (positive chirality), the first and second halves (the longer and shorter wavelength

(13) In (*S*)−(*M*)-**1f**, (*S*) stands for the absolute configuration of the sp^3 carbon at the 13 position, which was derived from the chiral carbon in **3f**, and (*M*) denotes the helicity of the conjugated aromatic plane.

(14) For a recent review of microwave-assisted organic synthesis, see: (a) *Microwave-Enhanced Chemistry*; Kingston, H. M., Haswell, S. J., Eds.; American Chemical Society: Washington, DC, 1997. (b) *Microwaves in Organic Synthesis*; Loupy, A. Eds.; Wiley-VCH: Weinheim, 2002. (c) Caddick, S. *Tetrahedron* **1995**, *51*, 10403. Loupy, A.; Perreux, L.; Liagre, M.; Burle, K.; Moneuse, M. *Pure Appl. Chem.* **2001**, *73*, 161. (d) Varma, R. S. *Pure Appl. Chem.* **2001**, *73*, 193. (e) Lidstrom, P.; Tierney, J.; Wathey, B.; Westman, J. *Tetrahedron*, **2001**, *57*, 9225. (f) Leadbeater, N. E.; Marco, M. *J. Org. Chem.* **2003**, *68*, 5662.

(15) 9-Substituted acridines were recently synthesized by microwave irradiation; see: (a) Veveková, E.; M. Nosková, M.; Toma, S. *Synth. Commun.* **2002**, *32*, 729. (b) Koshima, H.; Kutsunai, K. *Heterocycles* **2002**, *57*, 1299. (c) Seijas, J. A.; Vazquez-Tato, M. P.; Martinez, M. M.; Rodriguez-Parga, J. *Green Chem.* **2002**, *4*, 390.

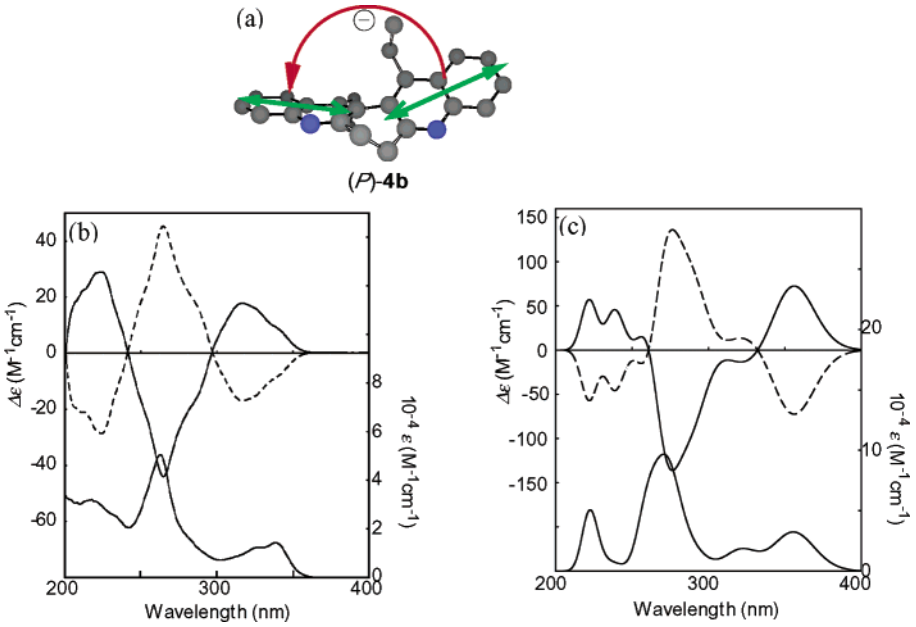

FIGURE 6. (a) Molecular geometry of (*P*)-**4b**: two green arrows represent electric transition dipole moments along the long axes of the quinoline chromophores, and a red arrow refers to the negative exciton chirality or the left-handed screwness between the two long axes of chromophores. (b) CD spectra (top) of optically resolved **4b**: first eluate (solid), second eluate (dotted).[10] Absorption spectrum (bottom) of **4b**. (c) Theoretical CD spectra (top) of (*P*)-**4b** (solid line) and (*M*)-**4b** (dotted line). Theoretical absorption spectrum (bottom) of **4b**. Scale on the right abscissa is for the absorption spectrum.

halves) of the split CD curve are positive and negative, respectively. With negative chirality, the first and second halves are negative and positive, respectively. The CD exciton chirality method seems to be applicable to **4** since **4** comprises two independent and equivalent quinoline moieties.[17] CD and UV−vis spectra of a pair of enantiomers of **4b** are shown in Figure 6b. Absorption of moderate intensity around 330 nm and a very intense absorption at 263 nm were distinguishing features of the UV−vis spectrum. These two are attributable to two transitions that are polarized along the short and long axes of the quinoline chromophore, respectively, and correspond to ^1L_a and ^1B_b transitions in a naphthalene ring. The latter is suited for observing the exciton coupling Cotton effect due to the large molecular extinction coefficient (ϵ) and the established assignment of the polarization of the transition. The strong negative Cotton effect at 265 nm for the first eluate of **4b**, depicted in Figure 6b as the solid line, may be assignable to the negative first split CD at the long-axis transition band. This anticipates the left-handed screwness between the two long axes of the chromophores and the provisional absolute configuration of (*P*)-helicity.[17] However, the distinct second split CD at this band could not be observed: obviously there are other transitions overlapping with the long-axis transition of quinoline chromophores. Therefore, considerable ambiguity remains in determining the absolute configuration of **4** by the CD exciton chirality method.[18]

Theoretical simulations reproducing CD spectra were accomplished to prove the above.[19] The molecular geometries obtained from single-crystal X-ray analyses (**1a**, **1b**, and **1f**) and from the geometry optimization with MM3 followed by MOPAC/PM5 (**4b**, Figure 6a) were adopted for the following calculations. The rotatory strengths for all excited states were calculated using the time-dependent density functional theory (TDDFT) with the B3LYP hybrid functional and the 6-31G(d,p) basis set. Calculations were carried out using the Gaussian 03 suite of programs.[20] We obtained the rotatory strengths from the dipole−length expression as well as the dipole−velocity expression for all the molecules.[19] Both rotatory strengths are the same for the exact wave functions for the ground and excited states concerned and should be close to each other for good wave functions. We used the former strengths to simulate spectra because the former strengths are essentially the same values as the latter strengths. Theoretical CD spectra were synthesized with the sum of Gaussian bands with the width of 0.18 eV. All calculated excitation energies are blue-shifted by 0.28 eV, and the intensities have been scaled by a factor of 0.5.[21] The theoretical CD spectra for a pair of enantiomers of **4b** are illustrated in Figure 6c. The theoretical UV−

(16) (a) Harada, N.; Nakanishi, K. In *Circular Dichroic Spectroscopy: Exciton Coupling in Organic Stereochemistry*; University Science Books: Mill Valley, CA, 1983. (b) Berova, N.; Nakanishi, K. In *Circular Dichroism, Principles and Applications*; Nakanishi, K.; Berova, N.; Woody, R., Eds.; VHC: New York, 1994. (c) Rodger, A.; Nordén, B. In *Circular Dichroism and Linear Dichroism*; Oxford, Oxford, New York, 1997.

(17) Provisional assignment of absolute configuration of **4a** in our previous communication (ref 4) was incorrect. We previously misjudged the direction of screwness between two long axes of the chromophores. For CD spectra of molecules possessing identical orientation of two chromophores to **4a**, see: (a) Imajo, S.; Nakamura, A.; Shingu, K.; Kato, A.; Nakagawa, M. *J. Chem. Soc., Chem. Commun.* **1979**, 867. (b) Imajo, S.; Kato, A.; Shingu, K.; Kuritani, H. *Tetrahedron Lett.* **1981**, *22*, 2179. (c) Shingu, K.; Imajo, S.; Kato, A.; Kuritani, H. *J. Am. Chem. Soc.* **1982**, *104*, 4272.

(18) For a review of the limitations of the CD exciton chirality method, see: Superchi, S.; Giorgio, E.; Rosini, C. *Chirality* **2004**, *16*, 422.

(19) (a) Grimme, S.; Harren, J.; Sobanski, A.; Vögtle, F. *Eur. J. Org. Chem.* **1988**, *53*, 1. (b) Furche, F.; Ahlrichs, R.; Wachsmann, C.; Weber, E.; Sobanski, A.; Vögtle, F. Grimme, S. *J. Am. Chem. Soc.* **2000**, *122*, 1717.

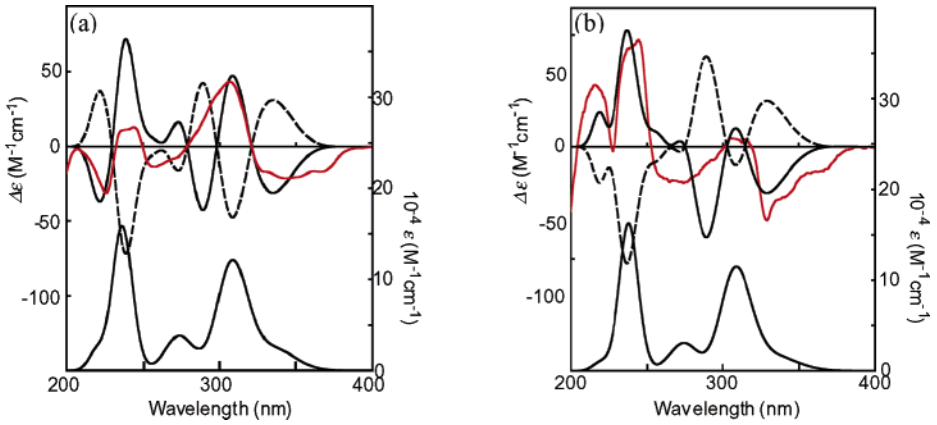

FIGURE 7. (a) Theoretical CD spectra (top) of (*P*)-**1a** (solid line) and (*M*)-**1a** (dotted line). Experimantal CD spectrum of the first eluate of **1a** (red). Theoretical absorption spectrum (bottom) of **1a**. (b) Theoretical CD spectra (top) of (*R*)−(*P*)-**1f** (solid line) and (*S*)−(*M*)-**1f** (dotted line). Experimantal CD spectrum of the first eluate of **1a** (red). Theoretical absorption spectrum (bottom) of **1f**. Scale on the right abscissa is for the absorption spectrum.

vis and CD spectra are highly resolved as compared with experimental ones and thus consist of several isolated bands. However, the theoretical CD spectrum of (*P*)-**4b** is approximately composed of three areas as in the experimental CD of the first eluate of **4b**: a positive band at 338 nm followed by intense negative bands around 277 nm and positive bands around 234 nm. Therefore, the experimental CD spectra are well reproduced by the calculation, and thus we have finally assigned the absolute configuration of the first eluate of **4b** as (*P*)-helicity. In this way we have also compared experimental and theoretical CD spectra of **1a**, **1b**, and **1f** and found that all experimental spectra were well described by calculation. Theoretical CD spectra of **1b** and **1f** along with the experimental ones are shown in Figures 7a and 7b, respectively.

Reduction of **1b** with $LiAlH_4$ seems possible to take place to produce **4b** with retention of helicity due to the high racemization barriers for **1b** and **4b** (Table 2). The first eluate of **1b**, which possesses the same CD signs as those of the first eluate of **1a** illustrated in Figure 3,[10] was collected (% ee ≥ 80%) and reduced by $LiAlH_4$ at room temperature to selectively yield the first eluate of **4b** (% ee ≈ 80%). These indicated that the absolute configrations of the first and second eluates of **1b** were (*P*)- and (*M*)-helicity, respectively. We have concluded from experimental and theoretical results that all of the first and second eluates in Figure 1 have absolute configurations of (*P*)- and (*M*)-, respectively.

Conclusion

We have demonstrated that novel helical aromatics were readily synthesized from commercially available compounds via one step. Microwave irradiation achieved shortening of the reaction period as well as brought about stereoselectivity in the synthesis of the helical aromatics. Of particular importance is also that the unusual stability against racemization in the helical aromatic formed from 2-methylglutaric acid is comparable to those of more widely known helicenes.[22] We have proven that theoretical CD generated by TDDFT derived the identical absolute configuration for helical aromatics. Thus, the theoretical CD spectra are reliable and will aid in the assignment of absolute configurations of not only helical molecules but also chiral molecules possessing sp^3 chiral genetic centers.

Experimental Section

General Procedure for Microwave-Assisted and Conventional Heating Reactions. We adopted a domestic microwave oven of MARUMAN MD-668 (2.54 GHz, 500 W fixed, 100 V, 60 Hz) produced in Japan in 1993. The microwave oven has been modified according to the literature.[23] Thus, we bore a hole of 2 cm in diameter at the very center of the top plate of the oven for the condenser fitting or measurement of the infrared radiation as an index of the reaction temperature. No leakage of microwaves has been detected using an electromagnetic field meter. A mixture of *N*,*N*′-*p*-phenylenediamine (**2**) (0.795 mmol), carboxylic acid (3.00 mmol), and zinc chloride (11.63 mmol) in a rounded-bottom flask equipped with or without a reflux condenser was placed in a domestic microwave oven (2.45 GHz, 500 W), and the sample was

(20) Frisch, M. J.; Trucks, G. W.; Schlegel, H. B.; Scuseria, G. E.; Robb, M. A.; Cheeseman, J. R.; Montgomery, J. A., Jr.; Vreven, T.; Kudin, K. N.; Burant, J. C.; Millam, J. M.; Iyengar, S. S.; Tomasi, J.; Barone, V.; Mennucci, B.; Cossi, M.; Scalmani, G.; Rega, N.; Petersson, G. A.; Nakatsuji, H.; Hada, M.; Ehara, M.; Toyota, K.; Fukuda, R.; Hasegawa, J.; Ishida, M.; Nakajima, T.; Honda, Y.; Kitao, O.; Nakai, H.; Klene, M.; Li, X.; Knox, J. E.; Hratchian, H. P.; Cross, J. B.; Adamo, C.; Jaramillo, J.; Gomperts, R.; Stratmann, R. E.; Yazyev, O.; Austin, A. J.; Cammi, R.; Pomelli, C.; Ochterski, J. W.; Ayala, P. Y.; Morokuma, K.; Voth, G. A.; Salvador, P.; Dannenberg, J. J.; Zakrzewski, V. G.; Dapprich, S.; Daniels, A. D.; Strain, M. C.; Farkas, O.; Malick, D. K.; Rabuck, A. D.; Raghavachari, K.; Foresman, J. B.; Ortiz, J. V.; Cui, Q.; Baboul, A. G.; Clifford, S.; Cioslowski, J.; Stefanov, B. B.; Liu, G.; Liashenko, A.; Piskorz, P.; Komaromi, I.; Martin, R. L.; Fox, D. J.; Keith, T.; Al-Laham, M. A.; Peng, C. Y.; Nanayakkara, A.; Challacombe, M.; Gill, P. M. W.; Johnson, B.; Chen, W.; Wong, M. W.; Gonzalez, C.; Pople, J. A. *Gaussian 03*, revision B.01; Gaussian, Inc.: Pittsburgh, PA, 2003.

(21) Difference in wavelength and absorption coefficient between theoretical and experimental CD and absorption spectra was partly rationalized by solvent effects and the systematic underestimation of higher excitation energies in TDDFT; see ref 18 and: Bauernschmitt, R.; Ahlrichs, R. *Chem. Phys. Lett.* **1996**, *256*, 454.

(22) [6]Helicene exhibits kinetic parameters of $\tau_{1/2}$ = 106 min and $\Delta G^{\ddagger}$ = 156.3 kJ mol^{-1} at 200 °C. [7]- and [8]helicenes showed $\Delta G^{\ddagger}$ = 174.5 and 177.4 kJ mol^{-1} at 27 °C, respectively; see: (a) Martin, R. H.; Marchant, M. J. *Tetrahedron* **1974**, *30*, 347. (b) Janke, R. H.; Haufe, G.; Würthwein, E.-U.; Borkent, H. *J. Am. Chem. Soc.* **1996**, *118*, 6031. (c) Meier, H.; Schwertel, M.; Schollmeyer, D. *Angew. Chem., Int. Ed.* **1998**, *37*, 2110.

(23) Ni-i, T.; Matsumura, T.; Oka, T. *Kagaku to Kyouiku* **1993**, *41*, 278.

irradiated. The reaction mixture obtained was neutralized with aqueous ammonia followed by extraction with chloroform and subsequent column chromatography on silica gel with $CHCl_3$-ethyl acetate as the eluant gave **1**. The synthetic procedure of conventional heating reactions was almost identical with those of the microwave-assisted reactions described above, except for the use of an oil bath for heating.

Chiral Resolution and Kinetic Measurements. The chiral resolution was accomplished by passing the acetonitrile solution of racemic **1** through a HPLC chiral column (DAICEL, CHIRALCEL OJ-R, solvent = 3/7 acetonitrile/H_2O) in both analytical and preparative scales. Kinetic measurements for the racemization of optically pure **1a** were taken in 3/7 acetonitrile/H_2O by means of CD spectroscopy, $\Delta\epsilon$ at 308.5 nm being utilized for estimating the time course of [(*P*)- or (*M*)-**1a**] and [racemic-**1a**]. The conversion of optically pure (*P*)-**1a** into its racemate followed first-order kinetics of $d[(P)\text{-}\mathbf{1a}]/dt = -k_1[(P)\text{-}\mathbf{1a}] + k_{-1}[\text{racemic-}\mathbf{1a}]$. The rate constant of racemization ($k_1 = 8.55 \times 10^{-5}$ s^{-1} at 20 °C) gave kinetic parameters of $\tau_{1/2}$ and $\Delta G^{\ddagger}$ from the equations of $\tau_{1/2} = \ln 2/k_1$ and $-\Delta G^{\ddagger} = RT \ln(k_1 h/k_B T)$ where h and k_B referred to the Planck and Boltzmann constants, respectively.

General Procedure for Obtaining HOMO Densities and Theoretical Racemization Barriers ($\Delta\Delta H_f^0$). We have confirmed that the orbital coefficients, the most stable conformations, and $\Delta H_f{}^0$ values generated by three different methods of MOPAC/AM1, MOPAC/PM5, and the time-dependent density functional theory (B3LYP/6-31G*) were almost identical, so MOPAC/PM5 was utilized unless otherwise noted. The most stable conformation was thus primarily generated by MM3 followed by MOPAC/PM5, resulting in the orbital coefficients. The HOMO density is equal to the square of the orbital coefficient of the p_Z component. The most stable conformation generated was adopted as the initial conformation for the following calculations for obtaining the theoretical $\Delta\Delta H_f{}^0$ as an index of racemization barrier. A dihedral angle consisting of four atoms denoted by R, 13, 14, and R in the chemical structures of (*P*)-**1** of (*M*)-**1** in the Introduction was defined. We decreased the dihedral angle by 5° from the initial conformation, immobilized the angle, and then calculated the most stable conformation and its $\Delta H_f{}^0$ using MOPAC/PM5. We continued this procedure until the largest $\Delta H_f{}^0$ was obtained. When the dihedral angle was 0° the largest, $\Delta H_f{}^0$ was always provided in which the conformations of the helical aromatics take the C_s symmetry.[11] The difference in $\Delta H_f{}^0$ values between the initial and final conformations was taken as the theoretical racemization energy ($\Delta\Delta Hf^0$).

Crystal Structures. Crystal structures of **1a**, **4a**, and **5a** have been reported previously.[4] Crystallographic data of **1b** and **1f** were collected on a Rigaku Mercury/CCD AXIS-4 diffractometer with graphite monochromated Mo Kα radiation [γ(Mo Kα) = 0.71070 Å]. Data were collected and processed using CrystalClear (Rigaku).[24] All calculations were performed using the CrystalStructure crystallographic software package.[25] Structures were solved by direct methods and expanded using Fourier techniques.[26,27] The non-hydrogen atoms were refined anisotropically. Hydrogen atoms were refined using the riding model. The full-matrix least-squares refinement on F^2 was carried out.

Crystal data and structure refinement for **1b** ($C_{24}H_{20}N_2$): crystal size = 0.30 × 0.20 × 0.05 mm, fw = 336.42, temperature = −120 °C, monoclinic, *C*2/*c*, a = 23.220(6) Å, b = 9.111(2) Å, c = 16.230(4) Å, β = 90.176(7)°, V = 3433.6(14) Å^3, Z = 8, ρ_c = 1.30 Mg/m^3, R_1 = 0.057, wR_2 = 0.131, GOF = 1.005. For **1f** ($C_{24}H_{18}N_2$): crystal size = 0.15 × 0.20 × 0.05 mm, fw = 334.42, temperature = −100 °C, monoclinic, $P2_1/n$, a = 7.980(3) Å, b = 12.096(5) Å, c = 17.014(7) Å, β = 90.122(11)°, V = 1642.4(12) Å^3, Z = 4, ρ_c = 1.352 Mg/m^3, R_1 = 0.082, wR_2 = 0.2000, GOF = 1.000.

Supporting Information Available: ^{1}H NMR spectra of **1a**−**e**, **1g**, **4a**, **4b**, **5a**, **6a′**, **8c**, and **8c′**; high-resolution mass spectra of **1a**−**g**, **4a**, **4b**, **5a**, **6a′**, **8c**, and **8c′**; elemental analyses of **1a**, **1d**, **1f**, and **4a**; the Z-matrix and the total energy for **1a**, **1b**, **1d**−**f**, **4b**, **5a**, and **8a′** generated by an optimized geometry calculation in MM/MOPAC using MM3/PM5 parameters; crystallographic information file (CIF) for **1b** and **1f**. This material is available free of charge via the Internet at http://pubs.acs.org.

JO048858K

(24) *CrystalClear*; Rigaku Corporation: 1999. CrystalClear Software User's Guide; Molecular Structure Corporation: 2000. Pflugrath, J. W. *Acta Crystallogr.* **1999**, *D55*, 1718−1725.

(25) (a) *CrystalStructure 3.6.0: Crystal Structure Analysis Package*; Rigaku and Rigaku/MSC: The Woodlands, TX, 2004. (b) Watkin, D. J.; Prout, C. K.; Carruthers, J. R.; Betteridge, P. W. *CRYSTALS Issue 10*; Chemical Crystallography Laboratory: Oxford, UK, 1996.

(26) Sheldrick, G. M. *SHELX97*; 1997.

(27) Beurskens, P. T.; Admiraal, G.; Beurskens, G.; Bosman, W. P.; de Gelder, R.; Israel, R.; Smits, J. M. M.; *The DIRDIF-99 Program System, Technical Report of the Crystallography Laboratory*; University of Nijmegen: Nijmegen, The Netherlands, 1999.